Shape and structure for the low-lying states of the ^{80}Ge nucleus

A. Ait Ben Mennana,[1] R. Benjedi,[1] R. Budaca,[2] P. Buganu,[2,*] Y. El Bassem,[1,3] A. Lahbas,[1,4] and M. Oulne[1]

[1]*High Energy Physics and Astrophysics Laboratory, Department of Physics, Faculty of Science Semlalia, Cadi Ayyad University, P. O. B. 2390, Marrakesh 40000, Morocco*

[2]*Department of Theoretical Physics, Horia Hulubei National Institute for Physics and Nuclear Engineering, Reactorului 30, RO-077125, POB-MG6, Bucharest Magurele, Romania*

[3]*Research Team ERMAM, Polydisciplinary Faculty of Ouarzazate, Ibn Zohr University, Ouarzazate Box 638, Morocco*

[4]*ESMaR, Department of Physics, Faculty of Sciences, Mohammed V University in Rabat, Rabat 10000, Morocco*

(Received 22 December 2021; accepted 14 March 2022; published 31 March 2022)

The ground-state shape of the ^{80}Ge nucleus and its evolution for the lowest collective excited states have been investigated in the framework of the Bohr model in order to clarify if the shape coexistence phenomenon is present. The obtained results, which are largely in agreement with the most recent experimental data, indicate a prolate shape for the ground state, respectively a sudden switch to a more deformed prolate one for certain excited states. Also, the first-excited 0_2^+ state is found to be very high in energy, namely, at 2208 keV, being close to recent predictions made with shell-model calculations. Additionally, using the parameters fit for the few available experimental data for the ground band, the structure of the β and γ bands has been built to support future experiments.

DOI: 10.1103/PhysRevC.105.034347

I. INTRODUCTION

Recent experimental data [1,2] revealed no evidence for shape coexistence in the ground state of the ^{80}Ge nucleus. The first-excited 0_2^+ state seen in a previous experiment [3] at 639 keV, which otherwise supports the presence of such phenomena, is missing now, being in turn predicted close to 2000 keV [2], but not below 1200 keV [1] by shell-model calculations. There are also other studies, both theoretical and experimental, which, over time, have paid attention to the shape evolution within the isotopic chain of Ge and especially to the shape coexistence in ^{80}Ge [4–10]. Nevertheless, the subject still remains open as long as the position of the first-excited 0_2^+ state is not fully clarified and, consequently, further experiments and theoretical calculations are needed for more confidence. Therefore, for this purpose, a new approach is applied in the present work to investigate the low-lying states of ^{80}Ge, namely, the Bohr Hamiltonian with a sextic potential (BHSP) [11] guided by outcomes offered by the covariant density-functional theory (CDFT) [12–18]. The BHSP [11] has already been applied with success in describing shape coexistence and mixing phenomena in several nuclei such as ^{76}Kr [19], ^{72,74,76}Se [20], and ^{96,98,100}Mo [21], while quite recently both methods have been used together to evince the existence of the shape coexistence in the ground state of the ^{74}Kr and ^{74}Ge nuclei [22], being thus suitable to address this issue. Besides this question related to the presence of the shape coexistence in the ground state of ^{80}Ge, equally important would be to get the structure of the nonyrast states in terms of possible β and γ excitations, especially that such states are not yet observed, and to see if the shape coexistence and mixing phenomena show up in excited states. For this latter purpose, the BHSP is an appropriate approach because all this information can be extracted using its free parameters fit for the few available experimental data.

The plan of the work consists in two main sections, one in which the BHSP is briefly reviewed and another where numerical applications are made for the experimental data of ^{80}Ge, verifying the structure of the low-lying states with respect to the shape evolution as a function of spin. Also, a section is dedicated for underlying the main achievements of the present study.

II. BOHR HAMILTONIAN WITH SEXTIC POTENTIAL

The Bohr Hamiltonian has the following expression [23,24]:

$$H = -\frac{\hbar^2}{2B}\left(\frac{1}{\beta^4}\frac{\partial}{\partial\beta}\beta^4\frac{\partial}{\partial\beta} + \frac{1}{\beta^2\sin 3\gamma}\frac{\partial}{\partial\gamma}\sin 3\gamma\frac{\partial}{\partial\gamma}\right) + \frac{\hbar^2}{8B\beta^2}\sum_{k=1}^{3}\frac{\hat{L}_k^2}{\sin^2\left(\gamma - \frac{2}{3}\pi k\right)} + V(\beta,\gamma), \quad (1)$$

where β and γ are the intrinsic deformation coordinates, B is a constant mass parameter, and $\hat{L}_k$ are the angular-momentum projections in the intrinsic reference frame. In the present study is used the solution proposed in Ref. [20] to describe coexistence between spherical and axially symmetric deformed nuclei. In this case, after the separation of the variables and solving the resulting γ equation, one has the following

*buganu@theory.nipne.ro

equation for the β variable:

$$\left[-\frac{1}{\beta^4}\frac{\partial}{\partial\beta}\beta^4\frac{\partial}{\partial\beta}+\frac{W}{\beta^2}+v(\beta)\right]f(\beta)=\epsilon f(\beta), \quad (2)$$

where $\epsilon=(2BE)/\hbar^2$ and $v(\beta)=(2BV)/\hbar^2$ are the reduced energy and potential, while [20]

$$W=\frac{L(L+1)-K^2}{3}+6cn_\gamma. \quad (3)$$

In Eq. (3), L and K are the quantum numbers for the eigenvalues of the total angular momentum and its projection on the z axis, c is the parameter describing the harmonic potential in the γ variable, while n_γ is the quantum number quantifying the γ vibrations. An appropriate potential to describe coexistence and mixing between spherical and deformed shapes would be the sextic oscillator potential:

$$v_{\rm eff}(\beta)=\frac{2+W}{\beta^2}+\beta^2-a\beta^4+b\beta^6, \quad (4)$$

where the change of function $f(\beta)=\beta^{-2}g(\beta)$ has been introduced, leading to the above effective potential $v_{\rm eff}$. Here, a and b are free parameters following to be fit as a function of the available experimental data. The solution for Eq. (2) with the potential (4) is found through a diagonalization procedure [11,19,20] using as a basis states solutions for an infinite square well potential:

$$\tilde{f}_{vn}(\beta)=\frac{\sqrt{2}\beta^{-\frac{3}{3}}J_v(z_n^v\beta/\beta_w)}{\beta_w J_{v+1}(z_n^v)}, \quad (5)$$

where J_v are Bessel functions of first kind of index

$$v=\sqrt{\frac{L(L+1)-K^2}{3}+6cn_\gamma+\frac{9}{4}}, \quad (6)$$

and their zeros z_n^v, while β_w denotes the width of the infinite square potential. The boundary value is determined for each pair of parameters a and b at a value where the external curve of the sextic potential makes an angle of 0.5 degrees with the vertical wall of the square well potential. Consequently, the wave function for Eq. (2) is written as

$$f_{v,n_\beta}(\beta)=\sum_{n=1}^{n_{\rm max}}A_{vn}^{n_\beta}\tilde{f}_{vn}(\beta), \quad (7)$$

where $n_\beta=0,1,2,\ldots,n_{\rm max}-1$ is the β vibrational quantum number. One can remark from Eq. (6) that the ground and β bands are decoupled from the γ band. For example, by considering $n_\gamma=K=0$ one gets the energies for the ground and β bands, which depend only on the free parameters a and b, while for $n_\gamma=1$ and $K=2$ the first γ band is constructed using the additional parameter c. Finally, taking into account also the contribution to the wave function coming from the γ variable and the three rotation Euler angles, the quadrupole electromagnetic transitions are defined for this case [20]:

$$B\big(E2,LKn_\beta n_\gamma\rightarrow L'K'n'_\beta n'_\gamma\big)$$
$$=\left(\frac{3R^2Ze}{4\pi}\right)^2\beta_M^2\big(C^{L2L'}_{K,K'-K,K'}B^{LKn_\beta n_\gamma}_{L'K'n'_\beta n'_\gamma}G^{Kn_\gamma}_{K'n'_\gamma}\big)^2, \quad (8)$$

where C is a Clebsch-Gordan coefficient, while B and G are integrals over the β and γ variables. More details about the B and G integrals can be found in Ref. [20]. Here, β_M is a scaling parameter which relates the β variable to the quadrupole deformation as $\beta_2=\beta_M\beta$, while Z, R, and e are the charge number, the nuclear radius, and the electron charge, respectively. Another important quantity for the shape coexistence signature is the monopole transition:

$$\rho^2_{if}(E0)=\left(\frac{3Z}{4\pi}\right)^2\beta_M^4\langle f_{L_iK_in_{\beta i}n_{\gamma i}}|\beta^2|f_{L_fK_fn_{\beta f}n_{\gamma f}}\rangle^2, \quad (9)$$

especially connecting ground and excited 0^+ states. Here, f is given by Eq. (7).

Furthermore, the model introduced in the present section is applied to describe the shape and structure for the low-lying quadrupole collective states within the ^{80}Ge nucleus.

III. NUMERICAL APPLICATIONS

In the last years, an entire polemic was raised over the existence of the shape coexistence phenomenon in the ^{80}Ge nucleus [1–10]. Even if an absence of this phenomenon is outlined more and more, the fact that the first-excited 0^+ state is still unmeasured, respectively there is a lack of data for the ground and excited bands in this nucleus, the problem still preserves its great interest. Consequently, through this study, we propose an alternative investigation for ^{80}Ge with the purpose to shed more light on its structure.

Thus, in a first step, the CDFT [12–18] is applied for ^{80}Ge by looking for its ground-state deformation properties. The obtained information will be further used to choose the appropriate instance of the phenomenological Bohr model: γ stable or γ unstable. In Fig. 1, the potential-energy surface (PES) determined with two functionals, the density-dependent point-coupling (DD-PC) and the density-dependent meson-exchange (DD-ME), is represented in the (β_2,γ) plane. The corresponding analytical formalism and the adopted coupling constants are those detailed in Ref. [22]. As one can see, ^{80}Ge presents well-pronounced prolate shape ($\beta_2=0.16,\gamma=0^\circ$) in both parametrizations; that is, it has a confined $\beta_2\neq 0$ minimum in the γ shape variable. These results confirm the most recent experimental data [1,2], according to which there is no shape coexistence in the ground state of this nucleus.

Taking into account the above results offered by CDFT, the attention concerning the application of the BHSP is further focused on predicting the position in energy for the first-excited 0^+ state of the ^{80}Ge. This is done by considering a γ-stable version of the Bohr model with a sextic potential [20] and whose parameters are fit to the available experimental data for the ground band. The quantum-mechanical ground band is identified with the observed yrast band. The results would be of great interest, especially due to the fact that the 0_2^+ state has not been observed yet experimentally, only an indirect prediction being made based on the experimental data of its neighboring isotopes, respectively in shell-model calculations [1,2].

The experimental energy ratios $E(8_1^+)/E(2_1^+)$, $E(6_1^+)/E(2_1^+)$, and $E(4_1^+)/E(2_1^+)$ are fit against only the two parameters a and b of the sextic potential because, for these states, $n_\gamma=0$. The obtained values $a=0.026\,641\,53$

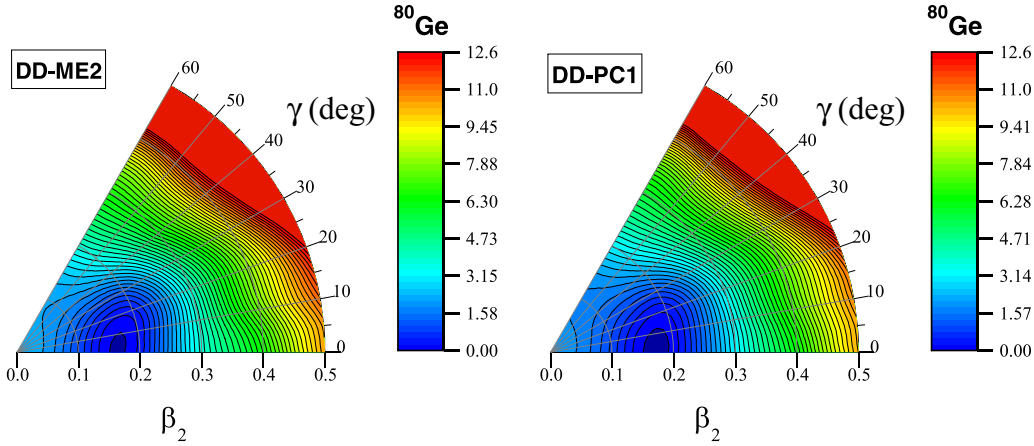

FIG. 1. Potential-energy surfaces for ^{80}Ge in the (β, γ) plane, obtained from a CDFT calculations with DD-ME2 and DD-PC1 parameter sets. The color scale shown at the right has the units of MeV and is scaled such that the ground state has a zero MeV energy.

and $b = 0.000\,203\,79$ correspond to the optimization value $\beta_w = 9.302$. For a more direct comparison between theory and experiment, one determines the scaling factor $\hbar^2/(2B) = 662.876$ keV by equating the theoretical and experimental energies for the first-excited state 2_1^+. An alternative procedure would be to fit the absolute energies of 8_1^+, 6_1^+, 4_1^+, and 2_1^+ experimental energy levels with a, b, and $\hbar^2/(2B)$, but the former scheme is preferable because it deals with scale-independent features of the model. The calculations are complemented by the transition probabilities, where one used the already fitted parameters a and b, as well as a scaling factor $\beta_M^2 = 0.012\,124\,3$ W.u., which is fit from the two experimentally available $B(E2)$ values. The corresponding theoretical energy spectrum, respectively the quadrupole $(E2)$ and monopole $(E0)$ transitions, are compared in Fig. 2 with the available experimental data [1,2,25]. The experimental data include some additional low-lying levels, which can be interpreted in the present model only as being part of a γ band. For the sake of completeness and as an additional test of the model, we fixed the parameter $c = 0.8565$ needed for the γ band states to reproduce the experimental 2_2^+ energy level and calculated a few more theoretical γ band states. The newly reported 3_1^+ and 4_2^+ states [1] can be considered as a possible experimental realization of the predicted γ-band extension. If further experimental studies confirm this band assignment, the irregular evolution of the experimental excitation energy within such a band can be theoretically reproduced by an appropriate treatment of anharmonicities in the γ variable [26] and its noncentrifugal coupling to the β shape variable [27]. Summing up the fitting procedure, there is always at least an additional data point to the number of parameters involved. First we have three energy ratios fit with two parameters, then we have a few more γ-band states predicted with the help of an additional c parameter, and finally fixing the scale β_M^2 one reproduces the relative difference between two experimental transition probabilities.

In an overview, one can remark that there is a very good agreement between all experimental energy levels and their theoretical counterparts. A special attention deserves the excellent reproduction of the $B(E2; 8_1^+ \rightarrow 6_1^+)$ transition which is very small compared with that from the first-excited state to the ground state. The result of interest refers to the energy of the first-excited 0^+ state, which is predicted to be at 2208 keV, being in agreement with the shell-model calculations made in Refs. [1,2]. Another signature for the presence of the shape coexistence phenomenon is the monopole transition between the first-excited 0^+ state and the ground state [28], which in our model is calculated and represented in Fig. 2 by the dashed arrow. This transition is usually enhanced when mixing is involved. Although being scale sensitive, the predicted value is quite sizable. This indicates a presence of a shape mixing rather than a coexistence of pure configurations [19]. To have a broader view over this problem, the next excited states of the β band are constructed above this 0^+ (2208 keV).

By looking carefully at these theoretical data obtained with BHSP, some apparently unusual behavior shows up for the highest states in energy. This structure can be easily clarified if one analyzes the plots presented in Fig. 3. For example, even if the effective potential presents two minima for $L = 0$, the energy level for the ground state is below the second minimum of the potential Fig. 3(a), while its corresponding density distribution probability of deformation has only a single peak centered somewhere around $\beta_2 = 0.16$ [Fig. 3(b)], a value predicted also by the CDFT. In the discussion that follows we will retain the index 1 for the ground-band states and use explicit β and γ subscripts for the corresponding theoretical bands. The next excited states, 2_1^+, 4_1^+, and 6_1^+, remain above the first minimum of the potential, following a displacement in deformation toward the second minimum of the potential, this being achieved for the 8_1^+ state for which the density distribution probability of deformation has a single peak above the second minimum of the potential. This sudden change in deformation between 6_1^+ and 8_1^+ explains the very small value (0.422 W.u.) for the $B(E2; 8_1^+ \rightarrow 6_1^+)$ transition experimentally observed. The point is that the two states are separated by the barrier, which makes them behave like they belong to two different bands, leading to small values for their matrix overlap elements, which otherwise are large in the absence of the barrier. A similar explanation can be given for

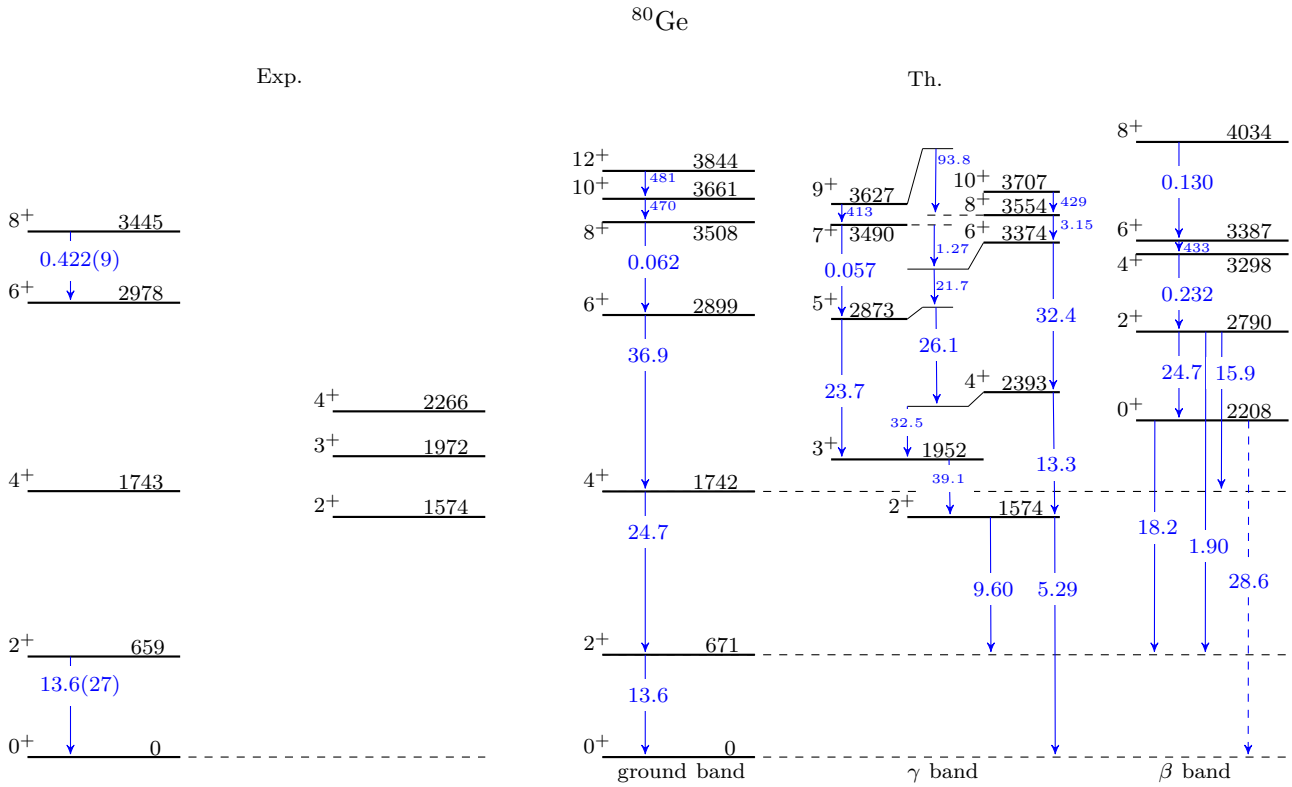

FIG. 2. Theoretical energy spectrum in keV, quadrupole transitions in W.u. (full arrows), and monopole transition $\rho^2(E0; 0_2^+ \rightarrow 0_1^+) \times 10^3$ (dashed arrow) compared with the available experimental data [1,2,25].

the β and γ bands as well. From Figs. 3(c) and 3(d), one can see that the states 0_β^+, 2_β^+, and 8_β^+ are positioned above the less deformed minimum, while 4_β^+ and 6_β^+ are above the second more deformed minimum of the potential. The states 4_β^+ and 6_β^+, being very close in energy, have almost indistinguishable plots for the density distribution probability and, because of that, only that for 4_β^+ has been plotted. Remark that the excited 4_β^+, 6_β^+, and 8_β^+ states do not exhibit the usual two-peak density distribution probability of deformation associated with β vibration. For $L = 4$ and 6, the β excited states act as ground states in the more deformed minimum, whereas, for $L = 8$, the situation is changed. This is the first example of shape coexistence without mixing realized in a Bohr model setting. Therefore, this change in shape toward the second minimum and turning to the first minimum explains the unusual variation of the $B(E2)$ transition in the β band. For the γ band, the shape changing starts with 7^+. An alternative investigation of this very unusual small $B(E2)$ value, otherwise experimentally observed in many nuclei [29–33], was given recently in Ref. [34] by using the interacting boson model [35] and assuming the states in this situation as being of collective nature, but having different motion modes. Therefore, the present result opens a door for many applications where such a behavior is observed.

At this point, it is instructive to discuss how the present phenomenological model reconciles with previous studies. Microscopic calculations revealed the importance of the $g_{9/2}$ neutron orbital for the correct reproduction of data in ^{80}Ge and its neighboring nuclei [1,2,36,37]. In lighter Ge isotopes, where shape coexistence is observed in the ground state, the $\nu g_{9/2}$ orbital is the target of the excited quasiparticle pairs. The harmonic-oscillator $N = 40$ shell gap is small, such that the corresponding energy levels come close to ground state and even mix with it [37]. Also, $N = 40$ marks the end of favorable nucleon numbers for the interplay between harmonic-oscillator and spin-orbit shell closures [38]. In the ^{80}Ge nucleus, the $\nu g_{9/2}$ orbital misses two neutrons to be completely filled, and the most energetically favorable quasiparticle excitations are from this orbital across the $N = 50$ spin-orbit shell gap, which is much larger than that at $N = 40$. This distinction inevitably pushes the quasiparticle configurations higher in energy and further from the ground state, as can be attested to by the systematics of low-lying energy levels in Ge isotopes [1,2,37]. This explains why a low-lying 0_2^+ state is a remote possibility.

The high-spin and intruder nature of the $g_{9/2}$ orbital produces a favorable condition for rotational antipairing effects. For example, the 8_1^+ state in ^{80}Ge is well understood as an isomeric $(\nu g_{9/2})^{-2}$ configuration [25,36]. This assignment is consistent with the backbending behavior of the experimental yrast spectrum, which is a consequence of the crossing between a regular rotational band (ground band) and another rotational band with a larger moment of inertia (S band) [39]. The structure of the second band is traditionally explained as being built on a broken nucleon pair with high single-particle spin alignments. Therefore, the 8_1^+ state would then be solely due to the alignment of two neutron $g_{9/2}$ holes. The S band can

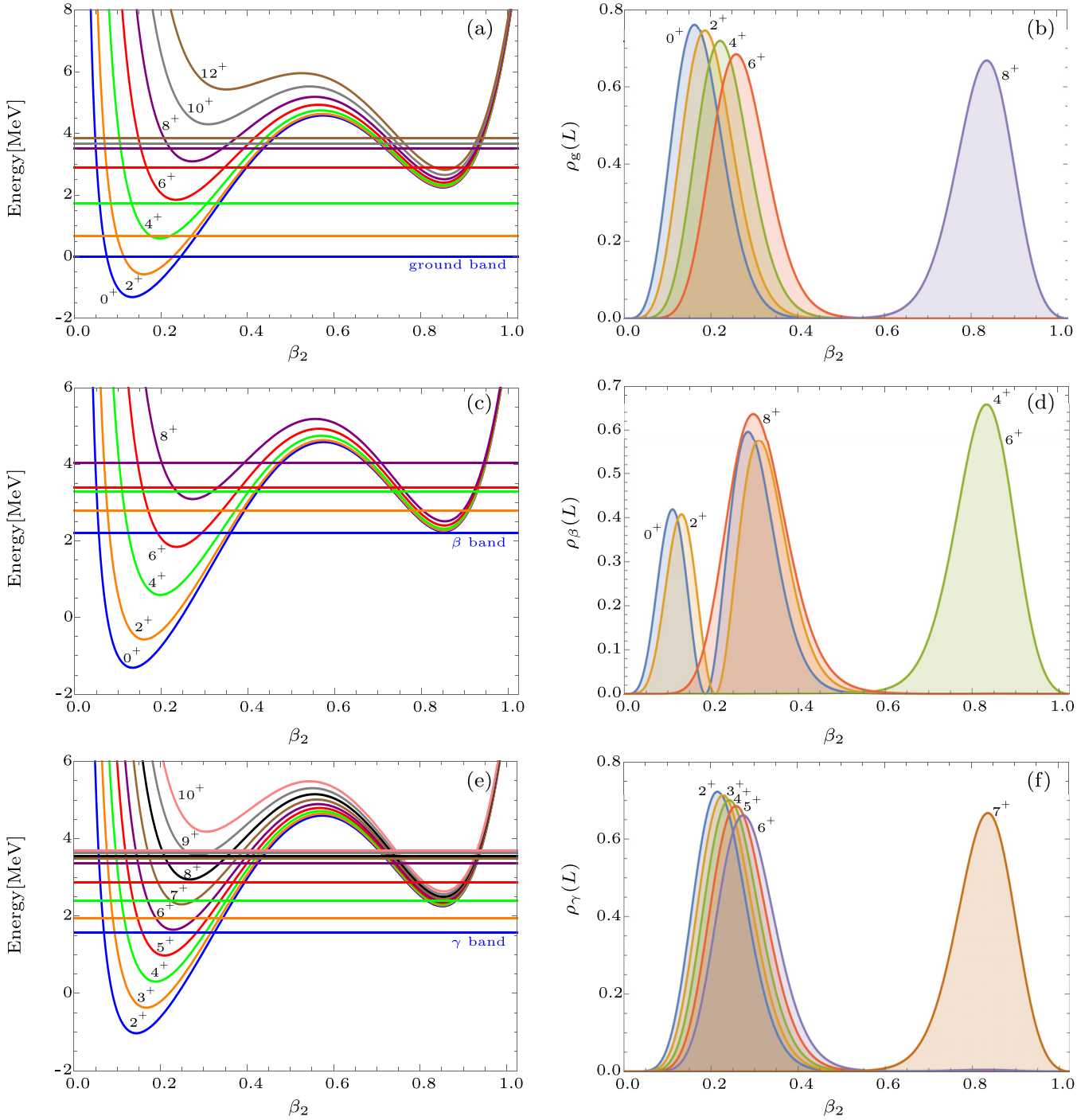

FIG. 3. Effective potential in the β variable, energy levels, and density distribution probability of deformation for the ground band [panels (a) and (b)], β band [panels (c) and (d)], respectively γ band [panels (e) and (f)].

also be interpreted as having a much larger deformation [39]. This image matches the present model calculation, where the high deformation minimum can be associated with the S band. Being of a different nature, the second minimum must be understood as an effective representation of the second rotational band (with quasiparticle alignments) in the same quantum space of deformation as the ground state. Hence, one has a very large deformation of the second potential minimum. This result is, however, consistent with the large deformation minimum forming at high spin states in the Hartree-Fock-Bogoliubov calculations [40] based on the Gogny force [41], which degenerates into a plateau at lower spin. The distinction between the microscopic and present phenomenological potentials for the low-lying states can be put to the restricted double-well shape defined by the simple sextic polynomial. We expect that a more general phenomenological potential will reproduce the data with a shallower and less deformed second minimum. The anomalous rotational sequence of the

experimental yrast band cannot be reproduced with an interpolation between standard collective vibrational and rotational spectra. Only adopting a two-well potential can such a feature be obtained, where a mixing between regular rotational spectra mix into a complex ground-state (yrast) band. As a matter of fact, even the experimental states of ^{80}Ge only up to 6_1^+ are anomalous enough such that a fit to only the two energy ratios with the present model lead to a double-well shape of the sextic potential. The phenomenology behind the double-well potential also explains the increase of experimental level density above the 8_1^+ state [1,25].

The similarity to the backbending phenomenon can be further exploited to draw some conclusions. The suggestions that even lower spin states have a similar structure [36], albeit with different alignments of the same $g_{9/2}$ holes, does not actually explain the hindering of the $B(E2, 8_1^+ \rightarrow 6_1^+)$ compared with the quite collective value of $B(E2, 2_1^+ \rightarrow 0_1^+) = 13.6(27)$. Microscopical calculations of the transition probabilities are conspicuously missing. As a matter of fact, in traditional backbenders from the rare-earth region, only the transition around the band-crossing point is hindered, due to the overlap between a fully collective state (with all particles paired) and a state with a broken pair [42]. This indicates that the 6_1^+ state is of different nature than the isomeric 8_1^+ state. The present model reproduction of the $B(E2, 8_1^+ \rightarrow 6_1^+)$ transition conforms to the simple backbending picture presented above. A similar mechanism was used to explain the intruder states in even-even Te nuclei [43] and the low-spin backbending in the ground band state of the ^{72}Se isotope [20]. The two potential minima of the present model act as the basis states in the two-level mixing model employed in shape coexistence and mixing studies [28,37,44]. Note, however, that here the two minima of the same potential describe the whole spectrum, unlocking the mixing between different configurations gradually by approaching the energy of the separation barrier. Moreover, the described mixing takes place in a well-understood space of deformation, rather than that of abstract coefficients weighting wave functions of different structure.

IV. CONCLUSIONS

The shape and structure for the lowest states of the ^{80}Ge nucleus were investigated in the framework of two approaches, namely, the covariant density-functional theory (CDFT) [12–18] and the Bohr Hamiltonian with sextic potential (BHSP) [11,19–22], for the β variable with the following results:

(i) A prolate shape is found for the ground state, which is in agreement with the most recent experiments [1,2], supporting the fact that there is no shape coexistence in the ground state for this nucleus. Instead, a possible shape mixing is suggested judging by the value calculated for the monopole transition between the first-excited 0^+ and the ground state.

(ii) The first-excited 0^+ state is found very high in energy at 2208 keV, which is in the limits predicted by recent shell-model calculations and indirect experimental observations [1,2].

(iii) The anomalous $B(E2; 8_1^+ \rightarrow 6_1^+)$ transition is very well reproduced in the frame of the BHSP by the fact that the two states have different β_2 deformation, being separated by a very high energy barrier. By this finding, a new mechanism of interpreting this behavior is proposed. This interpretation is in agreement with similar results obtained recently [34] involving calculations with the Interacting boson Model [35].

(iv) The structure of the β and γ bands have been constructed, coming in the help of future experiments and theoretical calculations. Shape coexistence of separate deformation configurations, which is without mixing, is predicted alternatively for $L = 4$, 6, and 8 states.

All these findings contribute to a better understanding of the structure for ^{80}Ge, a current challenging problem, but also open a door for many applications, there where some unusually small $B(E2)$ values are experimentally observed.

ACKNOWLEDGMENTS

This work was supported by High Energy Physics and Astrophysics Laboratory, Faculty of Science Semlalia, Cady Ayyad University-Marrakesh, Morroco and by Project PN-19-06-01-01/2019 of Romanian Ministry of Research, Innovation and Digitalization.

[1] S. Sekal, L. M. Fraile, R. Lica, M. J. G. Borge, W. B. Walters, A. Aprahamian, C. Benchouk, C. Bernards, J. A. Briz, B. Bucher, C. J. Chiara, Z. Dlouhy, I. Gheorghe, D. G. Ghita, P. Hoff, J. Jolie, U. Koster, W. Kurcewicz, H. Mach, N. Mărginean *et al.*, Phys. Rev. C **104**, 024317 (2021).

[2] F. H. Garcia, C. Andreoiu, G. C. Ball, A. Bell, A. B. Garnsworthy, F. Nowacki, C. M. Petrache, A. Poves, K. Whitmore, F. A. Ali, N. Bernier, S. S. Bhattacharjee, M. Bowry, R. J. Coleman, I. Dillmann, I. Djianto, A. M. Forney, M. Gascoine, G. Hackman, K. G. Leach *et al.*, Phys. Rev. Lett. **125**, 172501 (2020).

[3] A. Gottardo, D. Verney, C. Delafosse, F. Ibrahim, B. Roussiere, C. Sotty, S. Roccia, C. Andreoiu, C. Costache, M. C. Delattre, I. Deloncle, A. Etile, S. Franchoo, C. Gaulard, J. Guillot, M. Lebois, M. MacCormick, N. Mărginean, R. Mărginean, I. Matea *et al.*, Phys. Rev. Lett. **116**, 182501 (2016).

[4] E. Padilla-Rodal, O. Castaños, R. Bijker, and A. Galindo-Uribarri, Rev. Mex. Física S **52**, 57 (2006).

[5] L. Guo, J. A. Maruhn, and P.-G. Reinhard, Phys. Rev. C **76**, 034317 (2007).

[6] D. Verney, B. Tastet, K. Kolos, F. LeBlanc, F. Ibrahim, M. CheikhMhamed, E. Cottereau, P. V. Cuong, F. Didierjean, G. Duchene, S. Essabaa, M. Ferraton, S. Franchoo, L. H. Khiem, C. Lau, J. F. LeDu, I. Matea, B. Mouginot, M. Niikura, B. Roussiere *et al.*, Phys. Rev. C **87**, 054307 (2013).

[7] T. Nikšić, P. Marević, and D. Vretenar, Phys. Rev. C **89**, 044325 (2014).
[8] K. Nomura, R. Rodríguez-Guzmán, and L. M. Robledo, Phys. Rev. C **95**, 064310 (2017).
[9] D.-L. Zhang and C.-F. Mu, Chin. Phys. C **42**, 034101 (2018).
[10] S. Ahn, D. W. Bardayan, K. L. Jones, A. S. Adekola, G. Arbanas, J. C. Blackmon, K. Y. Chae, K. A. Chipps, J. A. Cizewski, S. Hardy, M. E. Howard, R. L. Kozub, B. Manning, M. Matos, C. D. Nesaraja, P. D. OMalley, S. D. Pain, W. A. Peters, S. T. Pittman, B. C. Rasco, M. S. Smith, and I. Spassova, Phys. Rev. C **100**, 044613 (2019).
[11] R. Budaca, P. Buganu, and A. I. Budaca, Phys. Lett. B **776**, 26 (2018).
[12] T. Nikšić, N. Paar, D. Vretenar, and P. Ring, Comput. Phys. Commun. **185**, 1808 (2014).
[13] G. A. Lalazissis, T. Nikšić, D. Vretenar, and P. Ring, Phys. Rev. C **71**, 024312 (2005).
[14] X. Roca-Maza, X. Viñas, M. Centelles, P. Ring, and P. Schuck, Phys. Rev. C **84**, 054309 (2011).
[15] T. Nikšić, D. Vretenar, P. Finelli, and P. Ring, Phys. Rev. C **66**, 024306 (2002).
[16] S. E. Agbemava, A. V. Afanasjev, D. Ray, and P. Ring, Phys. Rev. C **95**, 054324 (2017).
[17] Y. EL Bassem and M. Oulne, Nucl. Phys. A **987**, 16 (2019).
[18] Y. EL Bassem and M. Oulne, Int. J. Mod. Phys. E **28**, 1950078 (2019).
[19] R. Budaca and A. I. Budaca, Europhys. Lett. **123**, 42001 (2018).
[20] R. Budaca, P. Buganu, and A. I. Budaca, Nucl. Phys. A **990**, 137 (2019).
[21] R. Budaca, A. I. Budaca, and P. Buganu, J. Phys. G **46**, 125102 (2019).
[22] A. Ait Ben Mennana, R. Benjedi, R. Budaca, P. Buganu, Y. EL Bassem, A. Lahbas, and M. Oulne, Phys. Scr. **96**, 125306 (2021).
[23] A. Bohr, Mat. Fys. Medd. Dan. Vid. Selsk. **26**, 14 (1952).
[24] A. Bohr and B. R. Mottelson, Mat. Fys. Medd. Dan. Vid. Selsk. **27**, 16 (1953).
[25] B. Singh, Nucl. Data Sheets **105**, 223 (2005).
[26] M. A. Caprio, Phys. Rev. C **83**, 064309 (2011).
[27] D. J. Rowe, T. A. Welsh, and M. A. Caprio, Phys. Rev. C **79**, 054304 (2009).
[28] J. L. Wood, E. F. Zganjar, C. De Coster, and K. Heyde, Nucl. Phys. A **651**, 323 (1999).
[29] T. Grahn, S. Stolze, D. T. Joss, R. D. Page, B. Saygi, D. O'Donnell, M. Akmali, K. Andgren, L. Bianco, D. M. Cullen, A. Dewald, P. T. Greenlees, K. Heyde, H. Iwasaki, U. Jakobsson, P. Jones, D. S. Judson, R. Julin, S. Juutinen, S. Ketelhut *et al.*, Phys. Rev. C **94**, 044327 (2016).
[30] B. Sayği *et al.*, Phys. Rev. C **96**, 021301 (2017).
[31] B. Cederwall, M. Doncel, O. Aktas, A. Ertoprak, R. Liotta, C. Qi, T. Grahn, D. M. Cullen, B. S. NaraSingh, D. Hodge, M. Giles, S. Stolze, H. Badran, T. Braunroth, T. Calverley, D. M. Cox, Y. D. Fang, P. T. Greenlees, J. Hilton, E. Ideguchi *et al.*, Phys. Rev. Lett. **121**, 022502 (2018).
[32] A. Goasduff, J. Ljungvall, T. R. Rodriguez, F. L. Bello Garrote, A. Etile, G. Georgiev, F. Giacoppo, L. Grente, M. Klintefjord, A. Kusoglu, I. Matea, S. Roccia, M. D. Salsac, and C. Sotty, Phys. Rev. C **100**, 034302 (2019).
[33] D. Hertz-Kintish, L. Zamick, and S. J. Q. Robinson, Phys. Rev. C **90**, 034307 (2014).
[34] T. Wang, Europhys. Lett. **129**, 52001 (2020).
[35] F. Iachello and A. Arima, *The Interacting Boson Model* (Cambridge University Press, Cambridge, 1987).
[36] A. Makishima, M. Asai, T. Ishii, I. Hossain, M. Ogawa, S. Ichikawa, and M. Ishii, Phys. Rev. C **59**, R2331(R) (1999).
[37] K. Heyde and J. L. Wood, Rev. Mod. Phys. **83**, 1467 (2011).
[38] A. Martinou, D. Bonatsos, T. J. Mertzimekis, S. K. Peroulis, S. Sarantopoulou, and N. Minkov, Eur. Phys. J. A **57**, 84 (2021).
[39] P. Ring and P. Shuck, *The Nuclear Many-Body Problem* (Springer-Verlag, New York, 1980).
[40] http://www-phynu.cea.fr/science_en_ligne/carte_potentiels_microscopiques/noyaux/zz32/sep/zz32nn48sep_eng.html.
[41] S. Hilaire and M. Girod, Eur. Phys. J. A **33**, 237 (2007).
[42] R. Budaca and A. A. Raduta, J. Phys. G **40**, 025109 (2013).
[43] R. Budaca and A. I. Budaca, Eur. Phys. J. Plus **136**, 983 (2021).
[44] H. T. Fortune, Phys. Rev. C **99**, 054320 (2019).